Delft University of Technology

Delft Center for Systems and Control

Technical report 11-026

Reduction of area-wide emissions using an efficient model-based traffic control strategy*

S.K. Zegeye, B. De Schutter, J. Hellendoorn, and E.A. Breunesse

If you want to cite this report, please use the following reference instead:
S.K. Zegeye, B. De Schutter, J. Hellendoorn, and E.A. Breunesse, "Reduction of area-wide emissions using an efficient model-based traffic control strategy," *Proceedings of the 2011 IEEE Forum on Integrated and Sustainable Transportation Systems (FISTS 2011)*, Vienna, Austria, pp. 307–312, June–July 2011.

Delft Center for Systems and Control
Delft University of Technology
Mekelweg 2, 2628 CD Delft
The Netherlands
phone: +31-15-278.24.73 (secretary)
URL: `https://www.dcsc.tudelft.nl`

*This report can also be downloaded via `https://pub.deschutter.info/abs/11_026.html`

Reduction of Area-Wide Emissions Using an Efficient Model-Based Traffic Control Strategy

S. K. Zegeye, B. De Schutter, J. Hellendoorn, and E. A. Breunesse

Abstract— **In addition to the challenge to reduce traffic jams, reduction of traffic emissions in such a way that the dispersion of the emissions to residential areas, hospitals, schools, and other neighborhoods is decreased is a problem that requires state-of-the-art traffic control and management solutions. In this paper we model the dispersion of the emissions from a freeway traffic using a grid-based approach where the variability of the speed and direction wind is considered into account. The model is developed in such a way that the computation time is less than a previously proposed point-source model, while still capturing the important dispersion dynamics so that it can be used for on-line control applications. In order to reduce the dispersion of emissions to a neighborhood we design a parametrized model predictive control (MPC) strategy to optimize variable speed limits and ramp metering rates. We illustrate the proposed dispersion model and control approach with a simulation-based case study.**

I. Introduction

Emissions of road traffic, in general, are major contributors to the deterioration of the environment [4], [12], [19]. The global effect of these emissions is felt in the long run. In the short run (i.e. in the scale of seconds to minutes after the emissions are emitted) the neighborhoods of freeways are severely affected. There is a multitude of possible solutions for the long-run effect, such as improving vehicle technology and complete substitution of petroleum fuels by environmentally friendly ones. For the short-run effect, either the emissions have to be captured just after they are emitted or the traffic flow has to be controlled in such a way that the emissions are not dispersed to the public neighborhoods. This paper presents how traffic control measures can be used to reduce the dispersion of emissions to neighborhoods (predefined target areas).

In [24], we have developed a macroscopic emission model that takes the speed and acceleration of the traffic flow into account. In the paper [24] conventional MPC is employed to reduce the emissions, fuel consumptions, and travel time of the traffic. Although reduction of emissions contributes to the improvement of over all emission levels around the freeway, it does not necessarily mean that the emission levels on specific target zone is reduced.

Research supported by the Shell/TU Delft Sustainable Mobility program, the Transport Research Center Delft, the European COST Action TU0702, the European 7th Framework Network of Excellence "Highly-complex and networked control systems (HYCON2)", and the BSIK project "Next Generation Infrastructures (NGI)."

S. K. Zegeye, B. De Schutter, and J. Hellendoorn are with the Delft Center for Systems and Control, Delft University of Technology, Delft, The Netherlands. s.k.zegeye@gmail.com,{b.deschutter, j.hellendoorn}@tudelft.nl

E. A. Breunesse is with Shell Nederland B.V. The Hague, The Netherlands. ewald.breuness@shell.com

In an effort to demonstrate the potential of model predictive control (MPC) approaches to reduce dispersion of emissions to target areas, we have presented a simplified emission dispersion model in [25]. The paper [25] presents the use of variable speed limits to control the traffic flow so that the maximum dispersion level of the emissions at the target location is minimized. However, the model proposed in [25] assumed the speed and direction of the wind to be constant and it was based on a point-source modeling approach to model the dispersion, which could introduce large prediction errors. Since a conventional MPC approach is used in [25], the computation time is high. Thus it is difficult to use resulting MPC approach for on-line applications as it is meant to be.

In this paper, we first present a significantly extended and improved version of the emission dispersion model presented in [25]. The model incorporates the effect of varying wind speed and wind direction. Unlike [25], where a single point source is used to model the emissions from a freeway segment, here first the region around the freeway network traffic is divided into a grid of cells. All the emissions from the part of the freeway network in a given cell are next aggregated and assigned to that cell in a uniform way. Next the evolution of the emission level in each cell is modeled. Thus, the estimation of the emission levels in multiple target zones does not increase the computation time. Another contribution of the paper is a parametrized MPC control approach that is very fast and that provides almost the same performance as conventional MPC. The paper also illustrates the proposed model and control approach with a simulation-based case study.

This paper starts by discussing the traffic flow model and emission model in Section II and it continues by presenting the new grid-based dispersion model in Section III. In Section IV the proposed parametrized MPC is discussed. After presenting the case study in Section V, the paper concludes and presents topics for future work in Section VI.

II. Traffic flow and emission models

Since our control approach requires models to predict the traffic states (flow, speed, density, and emissions), in this section we provide the traffic flow and emission models we consider for this paper.

A. METANET

METANET [17] is a macroscopic second-order traffic flow model that describes the traffic behavior using aggregate variables. The macroscopic traffic variables are the density,

the flow, and the space-mean speed of the traffic flow. The model uses graph of nodes and links to represent traffic networks. A node is placed at a point where there is a change in the geometry of a freeway (such as a lane drop, an on/off-ramp, or a bifurcation). A homogeneous freeway that connects such nodes is represented by a link. A link is further divided into segments of length 500-1000 m [17]. The traffic dynamics in segment i of link m are given by

$$q_{m,i}(k) = \lambda_m \rho_{m,i}(k) v_{m,i}(k) \tag{1}$$

$$\rho_{m,i}(k+1) = \rho_{m,i}(k) + \frac{T}{L_m \lambda_m}\left[q_{m,i-1}(k) - q_{m,i}(k)\right] \tag{2}$$

$$\begin{aligned} v_{m,i}(k+1) = {} & v_{m,i}(k) + \frac{T}{\tau}\left[V[\rho_{m,i}(k)] - v_{m,i}(k)\right] \\ & + \frac{T v_{m,i}(k)\left[v_{m,i-1}(k) - v_{m,i}(k)\right]}{L_m} \\ & - \frac{T\eta\left[\rho_{m,i+1}(k) - \rho_{m,i}(k)\right]}{\tau L_m\left(\rho_{m,i}(k) + \kappa\right)} \end{aligned} \tag{3}$$

$$\begin{aligned} V[\rho_{m,i}(k)] = \min\Bigg\{ & (\alpha_m + 1) u_{m,i}(k), \\ & v_{\text{free},m} \exp\left[-\frac{1}{a_m}\left(\frac{\rho_{m,i}(k)}{\rho_{\text{cr},m}}\right)^{a_m}\right]\Bigg\} \end{aligned} \tag{4}$$

where $q_{m,i}(k)$, $\rho_{m,i}(k)$, and $v_{m,i}(k)$ denote respectively the flow, density, space-mean speed, and variable speed limit of segment i of link m at simulation step k, $v_{\text{free},m}$ denotes the free-flow speed, $u_{m,i}(k)$ denotes the variable speed limit, α_m denotes the drivers' compliance factor, L_m denotes the length of the segments of link m, λ_m denotes the number of lanes of link m, and T denotes the simulation time step size. Furthermore, $\rho_{\text{cr},m}$ is the critical density, and τ, η, a_m and κ are model parameters. The desired speed in (4) is obtained from [11].

For origins (such as on-ramps and mainstream entry points) a queue model is used. The dynamics of the queue length w_o at the origin o are modeled as

$$w_o(k+1) = w_o(k) + T\left(d_o(k) - q_o(k)\right) \tag{5}$$

where d_o and q_o denote respectively the demand and outflow of origin o. The outflow q_o is given by

$$\begin{aligned} q_o(k) = \min\Bigg[& d_o(k) + \frac{w_o(k)}{T},\ r_o(k) C_o, \\ & C_o\left(\frac{\rho_{\text{jam},m} - \rho_{m,1}(k)}{\rho_{\text{jam},m} - \rho_{\text{cr},m}}\right)\Bigg], \end{aligned} \tag{6}$$

with $r_o(k)$ the ramp metering rate (where $r_o \in [0\ 1]$ for a metered on-ramp and $r_o(k) = 1$ for an unmetered on-ramp or mainstream origin), $\rho_{\text{jam},m}$ the maximum density of link m, and C_o the capacity of the origin o. Refinements and extensions are discussed in [11], [17].

B. VT-macro

The VT-macro model [24] is a macroscopic emission model that is in particular developed for the METANET traffic flow model. The model takes the dynamics of the average space-mean speed of the traffic flow model into account. The inputs of the VT-macro model are the average space-mean speed, average acceleration, and the number of vehicles subject to the speed and acceleration pairs. These variables are computed from the space-mean speed, density, and flow variables of the METANET model.

The VT-macro model can be compactly described as

$$J_{y,m,i}(k) = f\left(v_{m,i}(k), v_{m,i}(k+1), v_{m,i+1}(k+1), \rho_{m,i}(k)\right) \tag{7}$$

where $J_{y,m,i}(k)$[kg/s] is the estimate or prediction of the emission variable $y \in \mathscr{Y} = \{\text{CO}, \text{CO}_2, \text{NO}_x, \text{HC}\}$ for segment i of link m during the time period $[kT, (k+1)T]$ and f is a nonlinear mapping (for a detailed discussion see [24]).

III. Grid-based dispersion modeling

There are several factors that affect the dispersion of vehicular emissions. In addition to the inherent characteristics of the emissions and geographical factors, wind and temperature are two important meteorological factors that play a significant role in characterizing the dispersion of emissions. In this paper we consider only the wind in modeling the dispersion of freeway traffic emissions, because, in general, the temperature varies slowly (in time and space) relative to the wind speed and wind direction. Therefore, we assume the temperature to be constant and hence its effects can be described (reflected) in the dispersion model as constant parameters. Moreover, we consider a constant flat terrain of the areas near the freeways and the meteorological conditions are assumed to be horizontally homogeneous. This means that the direction and speed of the wind responsible for transporting the plume from the emission source to the receptor (or target zone) and the turbulence responsible for diffusion are assumed not to change with location throughout the model domain. This is the same assumption made in straight-line Gaussian plume models and are presented explicitly in [16] and implicitly in [3], [6], [12].

The grid-based propagation of the emissions is modeled by extending the point-source dispersion model presented in [25]. To this end, we divide the region around the emission source into square cells of equal dimensions as in Fig. 1(a). In this figure the thick gray line represents a part of a freeway traffic network. The square regions of the grid are called cells and a cell is denoted by C_{i_c,j_c}, where the subscript i_c denotes the position of the cell in the x direction and j_c denotes the position of the cell in the y direction. A cell C_{i_c,j_c} in the grid space is described by the four corner points (x_{i_c}, y_{j_c}), (x_{i_c+1}, y_{j_c}), (x_{i_c+1}, y_{j_c+1}), and (x_{i_c}, y_{j_c+1}), where $x_{i_c} < x_{i_c+1}$ and $y_{j_c} < y_{j_c+1}$ (see also Fig. 1(b)).

Let the emission level in cell C_{i_c,j_c} (either the emission that was dispersed from the neighboring cells or the emission generated by the part of the freeway in the cell) for emission y at a time step k be denoted by $J_{y,i_c,j_c}(k)$. The emission in the cell is assumed to be uniformly distributed over the entire cell. The cell represents an infinite emission point sources. Now we consider each cell as consisting of an infinite collection of uniformly distributed point sources, and we apply the point-source model of [25]. Recall that we have assumed that the meteorological factors are horizontally homogeneous, the wind speed and wind direction does not

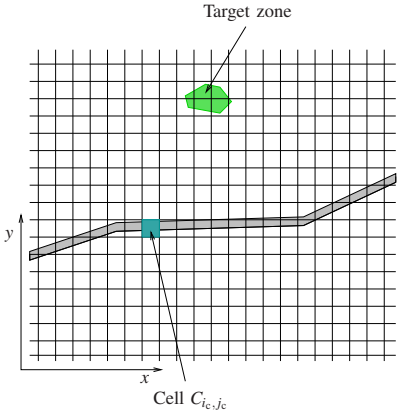

(a) Grid cells of the areas around a freeway.

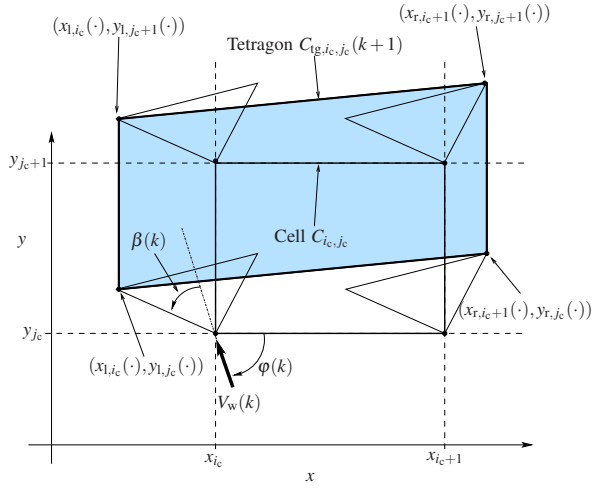

(b) Dispersion from cellC_{i_c,j_c}

Fig. 1. Schematic representation of area-source dispersion of emissions in 2D space.

vary within a cell. So, it is not important to trace the dispersion of all the point sources within the cell. In fact one only has to track the dispersion of the emissions at the boundary of the cells. The dispersion of the emissions within the cell will then remain within the newly formed dispersion zone. So, in our approach we track the dispersion of the emissions using the corner points of the grid cells. The dispersion of the emissions from each corner point of the cells is modeled as a point-source model. Each point source forms a dispersion cone as shown in Fig. 1(b). The derivation for the mathematical expressions of the dispersion cones can be found in [25]. Accordingly, the update rule for the point $(x_{l,i_c}(\cdot), y_{l,j_c}(\cdot))$ is for example given by

$$x_{l,i_c}(k+1) = x_{i_c}(k) + TV_w(k)\frac{\cos(\phi(k)-\beta(k))}{\cos(\beta(k)))} \quad (8)$$

$$y_{l,j_c}(k+1) = y_{j_c}(k) + TV_w(k)\frac{\sin(\phi(k)-\beta(k))}{\cos(\beta(k)))} \quad (9)$$

where $V_w(k)$ and $\phi(k)$ denote the wind speed and direction respectively, and $\beta(k) = \frac{\beta_{max}}{1+\beta_0 V_w(k)}$ with the maximum dispersion angle β_{max} at zero wind speed and β_0 a model parameter.

During the time period $[Tk,\ T(k+1)]$, the emissions $J_{y,i_c,j_c}(k)$ of cell C_{i_c,j_c} will propagate to the tetragon dispersion zone denoted by $C_{tg,i_c,j_c}(k+1)$. This is schematically represented in Fig. 1(b) with the light-blue/shaded area. The corner points of the tetragon $C_{tg,i_c,j_c}(k+1)$ are the points $(x_{l,i_c}(k+1), y_{l,j_c}(k+1))$, $(x_{r,i_c+1}(k+1), y_{r,j_c}(k+1))$, $(x_{r,i_c+1}(k+1), y_{r,j_c+1}(k+1))$, and $(x_{l,i_c}(k+1), y_{l,j_c+1}(k+1))$. As can be seen from Fig. 1(b), the tetragon is formed by joining the left-most and right-most points of the dispersion cones of the emissions from the corner points of the cell C_{i_c,j_c}. Note that both the cells C_{i_c,j_c} and the tetragon $C_{tg,i_c,j_c}(k)$ are polytopes so that their intersections[1] and its area can be computed easily and effectively [14].

Now let us denote the area of the dispersion tetragon $C_{tg,i_c,j_c}(k+1)$ be $A_{tg,i_c,j_c}(k+1)$ and the area of the cell C_{i_c,j_c} be A. The cell C_{i_c,j_c} has at most eight neighboring cells[2], namely: C_{i_c-1,j_c+1}, C_{i_c,j_c+1}, C_{i_c+1,j_c+1} to the top, C_{i_c-1,j_c} and C_{i_c+1,j_c} to the left and right respectively, and C_{i_c-1,j_c-1}, C_{i_c,j_c-1}, C_{i_c+1,j_c-1} to the bottom of the cell. Then, during the evolution of the emissions of cell C_{i_c,j_c}, the dispersion tetragon $C_{tg,i_c,j_c}(k+1)$ could intersect any of the neighboring cells and part of it can remain in the original cell C_{i_c,j_c}. Moreover, emissions from the neighboring cells can be dispersed to cell C_{i_c,j_c} depending on the wind speed, wind direction, and dispersion parameters. Therefore, the emission level $J_{y,i_c,j_c}(k+1)$ that will be accumulated in cell C_{i_c,j_c} during the time period $[Tk,\ T(k+1)]$ is given by

$$J_{y,i_c,j_c}(k+1) = J_{s,y,i_c,j_c}(k) + (1-\gamma(k)) \sum_{(u_c,v_c)\in\mathcal{N}(i_c,j_c)} \frac{\mathscr{A}(C_{i_c,j_c} \bigcap C_{tg,u_c,v_c}(k+1))}{A_{tg,u_c,v_c}(k+1)} J_{y,u_c,v_c}(k) \quad (10)$$

where $J_{s,y,i_c,j_c}(k)$ is the emission y generated by a source (e.g. vehicles in a freeway) in cell C_{i_c,j_c} at time step k, $\mathcal{N}(i_c,j_c)$ denotes the set of neighbors to cell C_{i_c,j_c} and the cell it self, $C_1 \bigcap C_2$ denotes the intersection of polytopes C_1 and C_2, $\mathscr{A}(C)$ denotes the area of the polytope C, $0 < \gamma(k) \leq 1$ denotes the factor that characterize the vertical dispersion of the emissions corresponding to cell C_{i_c,j_c}.

The emission levels at the target zone is therefore computed by summing up the fraction of the emissions contributed by each cell that intersect the target zone. Mathematically, the emission level for y at the target zone t at time step k is given by

$$D_{y,t}(k) = \sum_{(i_c,j_c)\in\mathcal{T}_{int,t}} \frac{\mathscr{A}(C_{target,t} \bigcap C_{i_c,j_c})}{A} J_{y,i_c,j_c}(k) \quad (11)$$

where $C_{target,t}$ denotes the polytope description of the target zone and $\mathcal{T}_{int,t}$ is the set of all cells in the grid that intersect the target zone t.

[1]This intersection is also a polytope.

[2]For stability reasons, the dimension of the cells should not be less than the distance moved by the emissions in one simulation time step. This is related to the CFL criterion encountered in [7]. Therefore, the number of cells that can disperse their emissions to the cell C_{i_c,j_c} will not exceed eight.

IV. Parametrized MPC

A. General concept

An MPC [20] controller uses a model of a system to predict the evolution of the state of the system for a sequence of control inputs using the current state of the system as the initial condition. Based on the predicted states of the system, the controller determines the value of a given cost function and optimizes the sequence of control inputs over the prediction horizon to minimize the cost function. Next, only the first control input of the optimal sequence is applied to the system until the next control time step, after which the controller repeats the above process all over again using a moving horizon principle.

MPC can handle nonlinear models, constraints, and multi-objective cost functions. Many traffic control researchers have shown that MPC can improve the performance of road networks [2], [11], [26]. Nonetheless, as a consequence of its high computation demands, MPC using advanced traffic models has not yet found its way to practice[3]. Some research work has already dealt with the reduction of the computation time (e.g. [10], [13], [15], [22]). However, the efforts were focusing on special systems, such as linear parameter-varying and linear time-varying systems. But, the traffic systems are too complex and nonlinear to fall within the specific classes of nonlinear systems for which the methodologies to reduce the computation time are developed.

For specific cases, one way to reduce the computation time of the MPC controller is to parametrize the control inputs using control law [5], [13], [15], [22]. For the cases considered there, the parametrization converts the non-convex optimization problem into convex one. But, this idea can only be used with certain class of systems. For our case, we parametrize the control inputs using control laws and parameters that are fewer than the number of control inputs. Then, at every control time step[4] k_c, the MPC controller optimizes the parameters of the control policy instead of the control inputs. In general, this option can improve the computation time. To illustrate this idea, in the sequel we present two traffic control measures and provide their parametrization using nonlinear state feedback control policies. Note that the parametrization is just an illustration of the control approach, but that the control approach is generic and it can also be used with other control laws and other control measures.

B. Control laws

We illustrate our approach using two traffic control measures, viz. variable speed limits and ramp metering rate. In conventional MPC, these two control measures would be optimized over the prediction horizon N_p directly. Now, in parametrized MPC the two control measures are determined according to control laws. The control laws of the variable speed limits and on-ramp metering rates can be defined in different ways. Here we give examples to just illustrate our approach.

The control law of the variable speed limits is defined using two nonlinear functions. One function describes the relative speed difference of a segment with respect to the speed of a downstream segment. The second is defined as the relative density difference of a segment with respect to the density of downstream segment. In both functions the relative difference between the current segment and the downstream segment of the freeway is used. This is because of the fact that drivers tend to adapt to the speed and density of vehicles in the downstream segments. Mathematically, the functions are given by

$$f_{1,m}(v_{m,i}(k_\mathrm{c}), v_{m,i+1}(k_\mathrm{c})) = \frac{v_{m,i+1}(k_\mathrm{c}) - v_{m,i}(k_\mathrm{c})}{v_{m,i+1}(k_\mathrm{c}) + \kappa_v}, \quad (12)$$

$$f_{2,m}(\rho_{m,i}(k_\mathrm{c}), \rho_{m,i+1}(k_\mathrm{c})) = \frac{\rho_{m,i+1}(k_\mathrm{c}) - \rho_{m,i}(k_\mathrm{c})}{\rho_{m,i+1}(k_\mathrm{c}) + \kappa_\rho}, \quad (13)$$

where κ_v and κ_ρ are fixed parameters introduced to prevent division by 0.

Using the function (12) and (13), the control law that parametrizes the variable speed limits is chosen to be

$$\begin{aligned} u_{\mathrm{sl},m,i}(k_\mathrm{c}+j+1) = {} & \theta_{0,m} v_{\mathrm{free},m} \\ & + \theta_{1,m} f_{1,m}(v_{m,i}(k_\mathrm{c}), v_{m,i+1}(k_\mathrm{c})) \\ & + \theta_{2,m} f_{2,m}(\rho_{m,i}(k_\mathrm{c}), \rho_{m,i+1}(k_\mathrm{c})) \end{aligned} \quad (14)$$

for $j = 0, 1, \ldots, N_\mathrm{p} - 1$.

The proposed parametrization has only 3 parameters (one could also vary $\theta_{\cdot,m}$ over the prediction horizon) to be optimized in the parametrized MPC control strategy. This means that the speed limit controller can reduce the computation time if it is used with a freeway that has more than three independent variable speed limits or more than three prediction horizon steps (since there are at least $3 \times N_\mathrm{p}$ speed limit variables over the prediction horizon).

Usually, the speed limits are constrained. The upper and lower bounds of the speed limit $L_\mathrm{l} \leq u_{\mathrm{sl},m,i}(k_\mathrm{c}+j) \leq L_\mathrm{u}$ for $j = 1, \ldots, N_\mathrm{p}$ can also be recast as constraints for the parametrization vector, where L_l and L_u are respectively the lower and upper speed limits.

Using a similar reasoning as for (13), we can define the parametrization of the ramp metering controller to be

$$u_{\mathrm{r},m,i}(k_\mathrm{c}+j+1) = u_{\mathrm{r},m,i}(k_\mathrm{c}+j) + \theta_{3,m} \frac{\rho_{\mathrm{cr},m} - \rho_{m,i}(k_\mathrm{c}+j)}{\rho_{\mathrm{cr},m}} \quad (15)$$

for $j = 0, 1, \ldots, N_\mathrm{p} - 1$.

Similar to the speed limit control, the constraint on the ramp metering rate $0 \leq u_{\mathrm{r},m,i}(k_\mathrm{c}+j) \leq 1$ for $j = 1, \ldots, N_\mathrm{p}$ can be translated into a constraint on the parameter $\theta_{3,m}$.

C. Performance measure

We consider a multi-objective performance criterion that accommodates the total time spent (TTS), total emission

[3] One could consider strategies like SCOOT [21] and UTOPIA/SPOT [23] to be MPC. But they only use very simple models.

[4] For the sake of simplicity we assume that the control step size T_c and the simulation step size T are related by $T_\mathrm{c} = MT$, for some positive integer M. Therefore, at time instant $t = k_\mathrm{c} T_\mathrm{c} = kT$ the control step counter k_c is an integer divisor of the simulation step counter k. They are then related by $k(k_\mathrm{c}) = Mk_\mathrm{c}$.

(TE), and the maximum dispersion level (DL) of emissions, as well as variations in time and space of the control signal. The multi-objective function is defined as a weighted sum of the constituents and it is given by

$$J(k_{\mathrm{c}}) = \zeta_1 \frac{\mathrm{TTS}(k_{\mathrm{c}})}{\mathrm{TTS}_{\mathrm{n}}} + \zeta_2 \frac{\mathrm{TE}(k_{\mathrm{c}})}{\mathrm{TE}_{\mathrm{n}}} + \zeta_3 \frac{\mathrm{DL}(k_{\mathrm{c}})}{\mathrm{DL}_{\mathrm{n}}} + \zeta_4 \Delta(k_{\mathrm{c}}) \tag{16}$$

where

$$\mathrm{TTS}(k_{\mathrm{c}}) = T \sum_{k=Mk_{\mathrm{c}}}^{M(k_{\mathrm{c}}+N_{\mathrm{p}})-1} \left(\sum_{(m,i)\in\mathscr{I}_{\mathrm{all}}} \lambda_m L_m \rho_{m,i}(k) + \sum_{o\in\mathscr{O}_{\mathrm{all}}} w_o(k) \right),$$

$$\mathrm{TE}(k_{\mathrm{c}}) = \sum_{y\in\mathscr{Y}} \mu_y \frac{\mathrm{TE}_y(k_{\mathrm{c}})}{\mathrm{TE}_{\mathrm{n},y}}, \qquad \mathrm{DL}(k_{\mathrm{c}}) = \sum_{y\in\mathscr{Y}} \mu_y \frac{\mathrm{DL}_y(k_{\mathrm{c}})}{\mathrm{DL}_{\mathrm{n},y}},$$

$$\Delta(k_{\mathrm{c}}) = \sum_{k=Mk_{\mathrm{c}}}^{M(k_{\mathrm{c}}+N_{\mathrm{p}})-1} \Bigg\{ \sum_{s\in\mathscr{S}_{\mathrm{all}}} \alpha_s \big(u_s(k) - u_s(k-1)\big)^2 + \sum_{(s_1,s_2)\in\mathscr{P}_{\mathrm{all}}} \alpha_{cs} \big(u_{s_1}(k) - u_{s_2}(k)\big)^2 \Bigg) + \sum_{r\in\mathscr{R}_{\mathrm{all}}} \alpha_r \big(u_r(k) - u_r(k-1)\big)^2 \Bigg\},$$

$$\text{with } \mathrm{TE}_y(k_{\mathrm{c}}) = \sum_{k=Mk_{\mathrm{c}}}^{M(k_{\mathrm{c}}+N_{\mathrm{p}})-1} \sum_{(m,i)\in\mathscr{I}_{\mathrm{all}}} J_{y,m,i}(k),$$

$$\mathrm{DL}_y(k_{\mathrm{c}}) = \sum_{t\in\mathscr{T}_{\mathrm{all}}} \max_{k=Mk_{\mathrm{c}},\ldots,M(k_{\mathrm{c}}+N_{\mathrm{p}})-1} D_{y,t}(k)$$

where $\zeta_i \geq 0$ for $i = 1,2,3,4$, and $\mu_y \geq 0$ are the weights, $\mathscr{O}_{\mathrm{all}}$ is the set of all origins in the traffic network, $\mathscr{I}_{\mathrm{all}}$ is the set of all segments of links in the traffic network, $\mathscr{S}_{\mathrm{all}}$ is the set of all speed limits, $\mathscr{P}_{\mathrm{all}}$ is the set of all consecutive speed limits, $\mathscr{T}_{\mathrm{all}}$ is the set of all target zones, and $\alpha_r = (\#(\mathscr{R}_{\mathrm{all}})N_{\mathrm{p}})^{-1}$, $\alpha_s = (\#(\mathscr{S}_{\mathrm{all}})N_{\mathrm{p}}v_{\mathrm{step}}^2)^{-1}$, and $\alpha_{cs} = (\#(\mathscr{P}_{\mathrm{all}})N_{\mathrm{p}}v_{\mathrm{step}}^2)^{-1}$ are the normalization factors of the ramp metering rate, the variation of the speed limits over time, and the variation of the speed limits is space respectively with v_{step} denoting a nominal maximum change of speed limit between different segments and time steps, and $\#(\cdot)$ denoting the set cardinality. Moreover, the subscript 'n' denotes nominal values of TTS, TE, TE_y, DL, and DL_y and these values are computed by simulating the uncontrolled traffic system with all speed limits set to $v_{\mathrm{free},m}$ and all on-ramp metering rates set to 1.

D. Optimization

The parametrized MPC optimization problem considered for this paper is nonlinear and non-convex. Thus a proper choice of an optimization technique has to be made in order to obtain feasible optimal control values. Owing to the non-convex nature of the objective function, global or multi-start local optimization methods are required. Hence, multi-start sequential quadratic programming [18, Section 5.3], pattern search [1], genetic algorithms [8], or simulated annealing [9] can be used.

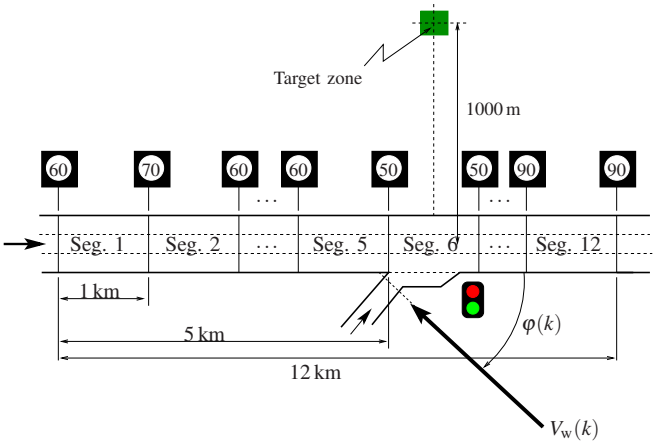

Fig. 2. A 12 km freeway with 12 variable speed limits and one on-ramp.

V. Case Study

A. Freeway set-up

To illustrate the applicability of the proposed grid-based dispersion model and the potential of the parametrized MPC control approach we consider a case study with a 12 km three-lane freeway stretch (see Fig. 2). The freeway is divided into 12 equal segments where each segment is controlled by a variable speed limit and with an on-ramp at the sixth segment. As target area for the dispersion we assume a school 1 km to the north of the freeway and 6 km away from the mainstream origin of the freeway.

We consider the freeway and its surroundings as being subject to wind with speed $V_{\mathrm{w}}(k) = 8 + 2\sin(0.005\pi k + \pi/6)\sin(0.01\pi k)$ and wind direction $\varphi(k) = \frac{2\pi}{5} + \frac{\pi}{4}\cos(0.004\pi k)$ where the wind speed $V_{\mathrm{w}}(k)$ is expressed in m/s and the wind direction (angle) $\varphi(k)$ in radians. Since the dispersion is assumed to be unobstructed (i.e. the meteorological factors are horizontally homogeneous), we consider the dispersion parameters as to be $\beta_{\max} = \pi$ and $\beta_0 = 0.9$. Moreover, the case study is simulated for an hour.

B. Performance measures

We consider the multi-objective function defined in (16). The system is simulated for uncontrolled and controlled cases. In particular, for the controlled cases we consider the objective function with $\mu_y = 1$ for all y and five different combinations of ζ_n for $n = 1,2,3,4$ (see Table I). In all these combinations $\zeta_4 = 0.01$, because we want to give less emphasis on the variation of the control inputs. The nominal values of the performance criteria are determined by simulating the uncontrolled traffic system with $v_{\mathrm{free},m} = 120$ km/h.

C. Results and discussion

The simulation results are shown in Table I and Fig. 3. The percentage reduction of the TTS, TE, or DL for the different control objectives are computed in comparison to the uncontrolled case. These values are depicted in Fig. 3.

TABLE I

SIMULATION RESULTS FOR DIFFERENT SCENARIOS.

Scenarios	Performance measure TTS [veh.h]	TE [kg]	DL [g]
S_0: Uncontrolled	1362.1	127.5	22.0
S_1: TTS	860.5	140.9	23.2
S_2: TE	1618.1	66.1	15.4
S_3: DL	1613.2	70.7	15.0
S_4: TE + DL	1543.8	68.5	15.5
S_5: 10TTS+TE+DL	1317.8	81.9	17.8

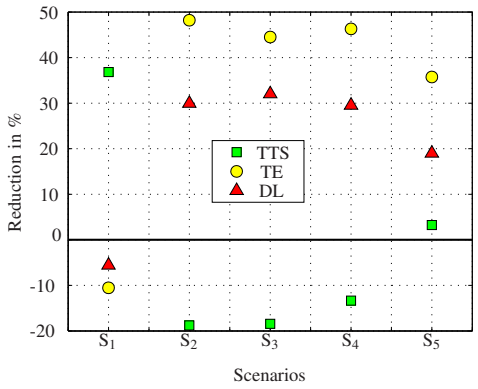

Fig. 3. Percentage reduction of traffic performance measures for different control objectives of the parametrized MPC relative to the uncontrolled scenario.

As can be seen from the Table I and Fig. 3 both the total emissions and the dispersion levels (total and maximum values) are worse if the objective of the controller is to reduce the travel time. Indeed the travel time is reduced by 37% (see Fig. 3). However, when the objective function of the controller is set either TE, DL, or the sum of TE and DL, the travel time increases by at least 13% while the TE and DL are reduced. The simulation results for the control objective $10\text{TTS} + \text{TE} + \text{DL}$ show that the controller provides reduced travel time, total emissions, as well as total and maximum dispersion levels of the emissions.

VI. CONCLUSIONS AND FUTURE WORK

We have presented an advanced and significantly extended version of previous point-source model. We have presented grid-based area-wide emission model that takes the effect of varying wind speed and wind direction. We have also discussed the parametrized MPC traffic control approach. We have illustrated the control approach and the area-wide emission model based on simulations.

In our future work, we will extend the model to consider the effect of temperature on the dispersion rate and compare the dispersion model with other models. Moreover, we will investigate the variation of the control measures and perform more extensive and complex case studies.

REFERENCES

[1] C. Audet and J. E. Dennis Jr. Analysis of generalized pattern searches. *SIAM Journal on Optimization*, 13(3):889–903, 2007.

[2] T. Bellemans, B. De Schutter, and B. De Moor. Model predictive control for ramp metering of motorway traffic: A case study. *Control Engineering Practice*, 14(7):757–767, July 2006.

[3] P. E. Benson. A review of the development and application of the CALINE3 and 4 models. *Atmospheric Environment*, 26B(3):379–390, September 1992.

[4] E. Brannvall and V. Špakauskas. Experimental and theoretical study of pollutant dispersion along a highway. *Geologija*, 60:27–32, 2007.

[5] A. Casavola, D. Famularo, and G. Franze. A predictive control strategy for norm-bounded LPV discrete-time systems with bounded rates of parameter change. *International Journal of Robust and Nonlinear Control*, 18(7):714–740, August 2007.

[6] D. P. Chock. A simple line-source model for dispersion near roadways. *Atmospheric Environment*, 12(4):823–829, 1978.

[7] R. Courant, K. Friedrichs, and H. Lewy. On the partial difference equations of mathematical physics. *IBM Journal of Research and Development*, 11(2):215–234, March 1967.

[8] L. Davis, editor. *Handbook of Genetic Algorithms*. Van Nostrand Reinhold, New York, USA, 1991.

[9] R. W. Eglese. Simulated annealing: A tool for operations research. *European Journal of Operational Research*, 46(3):271–281, 1990.

[10] P. J. Goulart, E. C. Kerrigan, and M. Maciejowski. Optimization over state feedback policies for robust control with constraints. *Automatica*, 42(4):523–533, April 2006.

[11] A. Hegyi, B. De Schutter, and H. Hellendoorn. Model predictive control for optimal coordination of ramp metering and variable speed limits. *Transportation Research Part C*, 13(3):185–209, June 2005.

[12] M. Khare and P. Sharma. Performance evaluation of general finite line source model for Delhi traffic conditions. *Transportation Research Part D: Transport and Environment*, 4(1):65–70, January 1999.

[13] M. V. Kothare, V. Balakrishnan, and M. Morari. Robust constrained model predictive control using linear matrix inequalities. *Automatica*, 32(10):1361–1379, 1996.

[14] M. Kvasnica, P. Grieder, and M. Baotić. Multi-Parametric Toolbox (MPT), 2004. `http://control.ee.ethz.ch/~mpt/`.

[15] J. Löfberg. Approximations of closed loop minimax MPC. In *Proceedings of the 42nd IEEE Conference on Decision and Control*, pages 1438–1442, Maui, Hawaii, USA, December 2003.

[16] S. A. McGuire, J. V. Ramsdell, and G. F. Athey. Rascal 3.0.5: Description of models and methods. Technical report, U.S. Nuclear Regulatory Commission, Washington, DC, USA, August 2007.

[17] A. Messmer and M. Papageorgiou. METANET: A macroscopic simulation program for motorway networks. *Traffic Engineering and Control*, 31(9):466–470, 1990.

[18] P. M. Pardalos and M. G. C. Resende. *Handbook of Applied Optimization*. Oxford University Press, Oxford, UK, 2002.

[19] K. S. Rao, R. L. Guner, J. R. White, and R. P. Hosker. Turbulence and dispersion modeling near highways. *Atmospheric Environment*, 36(27):4337–4346, September 2002.

[20] J. B. Rawlings and D. Q. Mayne. *Model Predictive Control: Theory and Design*. Nob Hill Publishing, Madison, Wisconsin, USA, 2009.

[21] D. I. Robertson and R. D. Bretherton. Optimizing networks of traffic signals in real time – the SCOOT method. *IEEE Transactions on Vehicular Technology*, 40(1):11–15, February 1991.

[22] R. S. Smith. Robust model predictive control of constrained linear systems. In *Proceedings of the 2004 American Control Conference*, pages 245–250, Boston, Massachusetts, USA, June 2004.

[23] Peek Traffic. Utopia/spot technical reference manual. Technical report, Reek Traffic, Amersfoort, The Netherlands, January 2002.

[24] S. K. Zegeye, B. De Schutter, J. Hellendoorn, and E. A. Breunesse. Model-based traffic control for balanced reduction of fuel consumption, emissions, and travel time. In *Proceedings of the 12th IFAC Symposium on Transportation Systems*, pages 149–154, Redondo Beach, California, USA, September 2009.

[25] S. K. Zegeye, B. De Schutter, J. Hellendoorn, and E. A. Breunesse. Variable speed limits for area-wide reduction of emissions. In *Proceedings of the 13th International IEEE Conference on Intelligent Transportation Systems*, pages 507–512, Funchal, Portugal, September 2010.

[26] J. Zhang, A. Boiter, and P. Ioannou. Design and evaluation of a roadway controller for freeway traffic. In *Proceedings of the 8th International IEEE Conference on Intelligent Transportation Systems*, pages 543–548, Vienna, Austria, September 2005.